Cell Reports

Article

Lack of functional TCR-epitope interaction is associated with herpes zoster through reduced downstream T cell activation

Graphical abstract

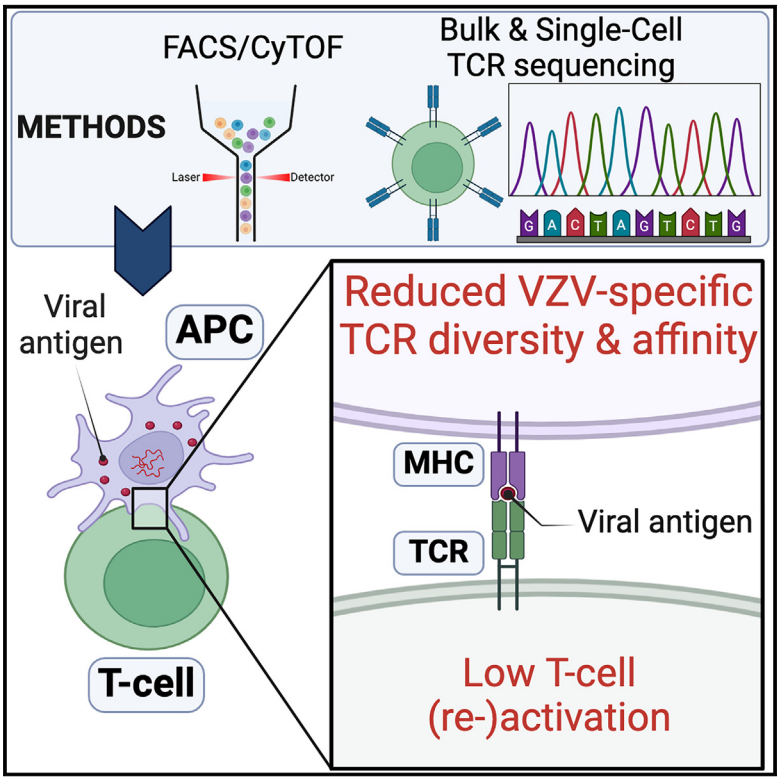

Highlights

- T cell phenotypes did not significantly differ between HZ patients and controls
- $CD4^+$ TCR diversity against VZV gE and IE63 after culture was broader in controls
- T cell activation pathways after VZV peptide stimulation were lower in HZ patients
- TCRs from HZ patients co-clustered more often together than TCRs from controls

Authors

Marlies Boeren, Nicky de Vrij, My K. Ha, ..., Kris Laukens, Pieter Meysman, Benson Ogunjimi

Correspondence

benson.ogunjimi@uantwerp.be

In brief

Boeren et al. demonstrate that susceptibility for shingles, caused by varicella-zoster virus (VZV) reactivation, correlates with reduced T cell receptor (TCR) diversity against several VZV proteins. Their results indicate that reduced T cell activation correlates with reduced affinity between VZV proteins and the VZV-specific TCR repertoire in shingles patients.

Boeren et al., 2024, Cell Reports *43*, 114062
April 23, 2024
https://doi.org/10.1016/j.celrep.2024.114062

CellPress

Cell Reports

CellPress
OPEN ACCESS

Article

Lack of functional TCR-epitope interaction is associated with herpes zoster through reduced downstream T cell activation

Marlies Boeren,[1,2,3,4,5,24] Nicky de Vrij,[4,6,7,8,24] My K. Ha,[3,4,5,24] Sebastiaan Valkiers,[4,6,7,24] Aisha Souquette,[9] Sofie Gielis,[4,6,7] Mariia Kuznetsova,[3,4,5] Jolien Schippers,[3,4,5] Esther Bartholomeus,[3,4,5] Johan Van den Bergh,[2] Nele Michels,[10] Olivier Aerts,[11] Julie Leysen,[11] An Bervoets,[11] Julien Lambert,[11] Elke Leuridan,[12] Johan Wens,[10] Karin Peeters,[3,4,5] Marie-Paule Emonds,[13] George Elias,[2,3,4,5] Niels Vandamme,[14,15] Hilde Jansens,[16] Wim Adriaensen,[8] Arvid Suls,[4,17] Stijn Vanhee,[18,19,20] Niel Hens,[4,5,21] Evelien Smits,[2,4,23] Pierre Van Damme,[4,12] Paul G. Thomas,[9] Philippe Beutels,[4,5] Peter Ponsaerts,[2] Viggo Van Tendeloo,[2,4] Peter Delputte,[1] Kris Laukens,[4,6,7,25] Pieter Meysman,[4,6,7,25] and Benson Ogunjimi[3,4,5,22,25,26,*]

[1]Laboratory of Microbiology, Parasitology and Hygiene (LMPH), University of Antwerp, Antwerp, Belgium
[2]Laboratory of Experimental Hematology (LEH), Vaccine and Infectious Disease Institute (VAXINFECTIO), University of Antwerp, Antwerp, Belgium
[3]Antwerp Center for Translational Immunology and Virology (ACTIV), Vaccine and Infectious Disease Institute, University of Antwerp, Antwerp, Belgium
[4]Antwerp Unit for Data Analysis and Computation in Immunology and Sequencing (AUDACIS), Antwerp, Belgium
[5]Centre for Health Economics Research and Modelling Infectious Diseases (CHERMID), Vaccine and Infectious Disease Institute, University of Antwerp, Antwerp, Belgium
[6]Adrem Data Lab, Department of Mathematics and Computer Science, University of Antwerp, Antwerp, Belgium
[7]Biomedical Informatics Research Network Antwerp (biomina), University of Antwerp, Antwerp, Belgium
[8]Clinical Immunology Unit, Department of Clinical Sciences, Institute of Tropical Medicine, Antwerp, Belgium
[9]Department of Immunology, St. Jude Children's Research Hospital, Memphis, TN, USA
[10]Department of Family Medicine and Population Health (FAMPOP), Center for General Practice/Family Medicine, University of Antwerp, Antwerp, Belgium
[11]Department of Dermatology, Antwerp University Hospital and University of Antwerp, Antwerp, Belgium
[12]Centre for the Evaluation of Vaccination (CEV), Vaccine and Infectious Disease Institute, University of Antwerp, Antwerp, Belgium
[13]Histocompatibility and Immunogenetic Laboratory, Rode Kruis-Vlaanderen, Mechelen, Belgium
[14]Data Mining and Modeling for Biomedicine Group, VIB-UGent Center for Inflammation Research, 9052 Ghent, Belgium
[15]Department of Applied Mathematics, Computer Science and Statistics, Ghent University, Ghent, Belgium
[16]Department of Clinical Microbiology, Antwerp University Hospital, Antwerp, Belgium
[17]Medical Genetics, University of Antwerp and Antwerp University Hospital, Antwerp, Belgium
[18]Laboratory of Immunoregulation and Mucosal Immunology, VIB Center for Inflammation Research, Ghent, Belgium
[19]Department of Internal Medicine and Pediatrics, Ghent University, Ghent, Belgium
[20]Department of Head and Skin, Ghent University, Ghent, Belgium
[21]I-BioStat, Data Science Institute, Hasselt University, Hasselt, Belgium
[22]Department of Paediatrics, Antwerp University Hospital, Antwerp, Belgium
[23]Present address: Center for Oncological Research (CORE), Integrated Personalized and Precision Oncology Network (IPPON), University of Antwerp, Antwerp, Belgium
[24]These authors contributed equally
[25]These authors contributed equally
[26]Lead contact
*Correspondence: benson.ogunjimi@uantwerp.be
https://doi.org/10.1016/j.celrep.2024.114062

SUMMARY

The role of T cell receptor (TCR) diversity in infectious disease susceptibility is not well understood. We use a systems immunology approach on three cohorts of herpes zoster (HZ) patients and controls to investigate whether TCR diversity against varicella-zoster virus (VZV) influences the risk of HZ. We show that $CD4^+$ T cell TCR diversity against VZV glycoprotein E (gE) and immediate early 63 protein (IE63) after 1-week culture is more restricted in HZ patients. Single-cell RNA and TCR sequencing of VZV-specific T cells shows that T cell activation pathways are significantly decreased after stimulation with VZV peptides in convalescent HZ patients. TCR clustering indicates that TCRs from HZ patients co-cluster more often together than TCRs from controls. Collectively, our results suggest that not only lower VZV-specific TCR diversity but also reduced functional TCR affinity for VZV-specific proteins in HZ patients leads to lower T cell activation and consequently affects the susceptibility for viral reactivation.

INTRODUCTION

Adaptive immunity forms our second line of defense and is, unlike innate immunity, defined by its specificity toward molecular structures on pathogens, i.e., antigens (mainly peptides).[1] Pathogen-derived antigens can be presented by cells on major histocompatibility complex class I (MHC I) molecules for recognition by T cell receptors (TCRs) on $CD8^+$ T cells that are capable of targeting the infected cell and use cytotoxic and/or cytolytic methods to combat the pathogen.[1,2] Conversely, antigen-presenting cells (APCs) can present peptides on MHC II molecules for recognition by TCRs on $CD4^+$ T cells.[1,2] $CD4^+$ T cells' main role consists of assisting in the generation of antibodies and $CD8^+$ T cells. Importantly, MHC I and II molecules are encoded by the respective classical human leukocyte antigen (HLA) genes -A, -B, -C, -DR, -DP, and -DQ.[3] After the development of T cells in an individual's thymus, the TCR repertoire will reflect the individual's MHC genetic constitution. The TCR variable domain CDR3 (complementarity determining region 3) is responsible for the recognition of the antigen-MHC complex, leading to the initiation of a $CD4^+$ or $CD8^+$ T cell response. Thus, importantly, depending on an individual's HLA genetic constitution, each individual will recognize a different set of peptides (or with different affinities), thereby adding to the factors that could render individuals susceptible to infections when these individuals are lacking pathogen-specific TCRs in their repertoire as indicated by HLA association studies. Furthermore, viral reactivations have also been noted to be associated with certain HLA alleles.[4]

A primary infection with varicella-zoster virus (VZV) causes chickenpox (varicella). After initial infection, VZV remains dormant in neural ganglia until it is reactivated, causing a condition called herpes zoster (HZ, shingles), which typically presents as a painful dermatomal rash. It is already well known that immunosenescence is associated with the development of HZ.[5] Indeed, HZ incidence increases with aging concurrent with a decline in VZV cell-mediated immunity (CMI).[6,7] However, HZ does not only occur in the elderly[5] but also frequently in immunocompromised patients[8] and healthy individuals.[9,10]

In Japanese patients, a meta-analysis showed that HLA-A*02 and HLA-B*40 were protective, whereas HLA-A*33 and HLA-B*44 were risk serotypes for a specific HZ complication, postherpetic neuralgia (PHN).[11] In addition, these risk factors were computationally associated with a lower affinity of VZV peptides for MHC I molecules, meaning that a higher risk for PHN was associated with lower binding affinities.[11] Importantly, it was suggested that PHN susceptibility was likely not caused by a lack of T cell response against one specific VZV antigen but by the aggregate inefficiency of VZV-specific T cell responses.[11] A Belgian pilot study including 50 individuals with a history of HZ and a control population of 25,000, showed that HLA-A*11 was associated with protection against HZ, whereas HLA-B*37 was a risk allele for the development of HZ.[12] Interestingly, computational models indicated that younger HZ patients had HLA variants with a lower affinity for VZV IE62, one of the proteins assumed to be of importance during VZV reactivation.[13] Finally, a recent genome-wide association study (GWAS) on more than 2,700 HZ cases and 130,000 controls showed HLA-A*01:01, HLA-B*07:02, HLA-B*40:01, and HLA-C*07:02 to be HZ risk alleles, whereas HLA-A*02:01, HLA-DRB1*11:01, HLA-DRB3*02:02, and HLA-DQB1*03:01 were noted to be HZ protective alleles.[14] Noteworthy, in a small cohort ($n = 7$), BK virus (BKV) clearance time after BKV reactivation in renal transplant patients was noted to be inversely correlated with BKV-specific TCR diversity.[15]

Given (1) that an HZ vaccination trial showed that VZV CMI prior to HZ is lower compared to VZV CMI in controls, thereby suggesting that VZV CMI is the main factor controlling symptomatic VZV reactivation,[16] and (2) the mentioned HLA VZV modeling data,[11–13] we hypothesized that restricted TCR diversity might be a risk factor for the development of HZ.

RESULTS

Mass cytometry shows no differences in mononuclear cell types and differentiation subsets between HZ patients and controls

First, we determined whether general differences in peripheral blood mononuclear cell (PBMC) composition were associated with the development of HZ by phenotyping unstimulated PBMCs using mass cytometry (CyTOF). PBMCs were obtained from 23 HZ patients 1 year after the HZ episode, and from 23 age- and gender-matched controls around the 1-year time point (cohort 1). Additionally, eight HZ patients donated PBMCs during the active HZ episode. The identified populations consisted of monocytes, natural killer (NK) cells, dendritic cells (DCs), B cells, naive $CD4^+$ and $CD8^+$ T cells, central memory (CM) $CD4^+$ and $CD8^+$ T cells, effector memory (EM) $CD4^+$ and $CD8^+$ T cells, and terminally differentiated effector memory (TEMRA) $CD4^+$ and $CD8^+$ T cells. Less abundant cell types were not detected in this assay due to the relatively low cell count. Importantly, we found no differences in the percentages of any of the aforementioned cell populations between HZ patients 1 year after the HZ episode and their matched controls (Figure S1). Likewise, no differences were found when comparing the percentage of these cell types during HZ and 1 year later (Figure S1).

HZ patients show increased VZV-specific antibody titers at least up to 1 year after the HZ episode compared to controls

Next, we compared VZV-specific antibody titers of HZ patients and controls during the acute episode (HZ), 1 year later (HZ1y), and controls (CO). As expected, VZV antibody titers were significantly higher in HZ patients during the HZ episode than in controls (Figure S2A). 1 year after the HZ episode, VZV antibody titers had significantly dropped but were still significantly higher compared to controls (Figure S2A). Furthermore, it was previously shown that cytomegalovirus (CMV) seropositivity was associated with HZ.[17,18] However, using a contingency table approach (Fisher's exact test) on the CMV serostatus of HZ patients and controls, we could not confirm this in the smaller cohort in this study (odds ratio = 1.65 with 95% confidence interval [0.62; 4.43]) (Figure S2B). In addition, we compared VZV antibody levels in each group (i.e., HZ, HZ1y, and CO) between CMV-negative and CMV-positive participants and did not find a significant difference (Figure S2C).

Frequencies of VZV-specific CD4$^+$ or CD8$^+$ T cells do not differ between HZ patients and controls

Given that previous studies suggested that VZV-specific CMI was lower in HZ patients, we specifically assessed the dynamics of VZV-specific CD4$^+$ and CD8$^+$ T cells in HZ patients and controls. To achieve this, the percentage of VZV-specific CD4$^+$ and CD8$^+$ T cells from 12 HZ patients was determined at active HZ (cohort 2) and consecutive time points after active disease and compared to 11 controls (without known re-exposure to VZV in the last year and without a history of HZ). Using intracellular cytokine staining, we found no difference regarding the percentage of IFN-gamma-producing CD4$^+$ or CD8$^+$ T cells against peptide pools VZV IE62, IE63, or gE, between the different time points for HZ patients (during HZ [T0] and 3 [T3], 6 [T6], 15 [T15], or 30 [T30] weeks after HZ) or between controls (CO) and any of the time points during HZ (T0) or after HZ (T3, T5, T15, and T30) (Figure S3). Likewise, no significant differences were observed in the percentage of IL-2 producing CD4$^+$ or CD8$^+$ T cells against any of the VZV peptides between any of the groups (Figure S4). Given the use of "only" two cytokines and the use of "only" three VZV proteins, we also compared, after stimulating PBMCs with either VZV lysate or VZV IE63, activation-induced marker (CD137$^+$CD69$^+$ for CD8$^+$ T cells; CD154$^+$OX40$^+$ for CD4$^+$ T cells) T cell frequencies between (1) HZ patients and controls at corresponding time points and (2) different time points from either HZ patients or controls. PBMCs were obtained from remaining cohort 1 and cohort 2 vials. As shown in Figure S5, no statistically significant differences were found between any of the conditions. Interestingly, when comparing T cell phenotype (CCR7$^-$CD45RA$^-$, CCR7$^-$CD45RA$^+$, CCR7$^+$CD45RA$^-$, CCR7$^+$CD45RA$^+$) and senescence/exhaustion markers (univariate Fas, TIGIT, CD27, CD28, LAG3) frequencies within activation-induced markers (AIM)-positive T cells between (1) HZ patients and controls at corresponding time points and (2) different time points from either HZ patients or controls, we only found differences regarding VZV lysate specific CD8$^+$ T cells and the percentages of CCR7$^+$CD45RA$^+$ T cells when comparing controls at baseline, controls after 1 year, HZ patients at baseline, and HZ patients after 1 year. Given the multitude of comparisons performed and the relatively low number of participants, we may consider these results to be rather an artifact.

From another cohort (cohort 3) approach, we also obtained single-time-point PBMCs from 10 individuals prior to their HZ onset (−23 days, −74 days, −153 days, −164 days, −226 days, −314 days, −341 days, −371 days, −465 days, −547 days) and 20 age- and gender-matched controls (thus without any previous or to be developed HZ). We stimulated their PBMCs with VZV lysate and VZV IE63 overnight and performed AIM quantification. Our results didn't show a significant difference between CO and pre-HZ participants regarding CD4$^+$ T cell nor CD8$^+$ T cell frequencies (see Figure S6). Like for cohorts 1 and 2, we looked again at T cell phenotypes and only noted IE63-specific CD4$^+$ T cells to have higher CCR7$^-$CD45RA$^+$ T cell frequencies in controls vs. pre-HZ patients.

Thus, in contrast to other studies, our study did not support the hypothesis that a lower total T cell count against VZV might be a key susceptibility factor for the development of HZ.

Total TCRβ count of VZV IE62, VZV IE63, and VZV gE specific CD4$^+$ or CD8$^+$ T cells also does not differ between HZ patients and controls

Given our hypothesis-revoking results, we challenged our own findings via an independent second assay where alternatively T cell activation was investigated through stimulation of PBMCs with VZV peptide pools (and a control influenza peptide pool), during a 1-week culture, after which sorting using CD71 and CD98 activation markers was performed, followed by TCRβ sequencing. PBMCs used in this assay were obtained from 23 HZ patients 1 year after the HZ episode and from 23 age- and gender-matched controls around the 1-year time point (cohort 1). Additionally, eight HZ patients donated PBMCs during the active HZ episode. We noted that the total TCRβ count of CD4$^+$ and CD8$^+$ T cells against VZV peptides gE, IE62, or IE63 was not significantly lower during the HZ episode (HZ) than 1 year after the HZ episode (HZ1y) and compared to controls (CO) and did not differ between HZ1y and CO (Figure 1). These data are in concordance with the data of the first method in which IFN-y production was assessed, showing no difference in the percentage of CD4$^+$ and CD8$^+$ T cells against VZV IE62, IE63, and gE between any of the groups. Thus, based on the data of these two independent and complementary methods, the total number of CD4$^+$ or CD8$^+$ T cells against selected specific VZV peptides was not associated with HZ. Noteworthy, stimulation with VZV lysate showed a significant difference between HZ and CO and between HZ and HZ1y in the CD4$^+$ T cell TCR count, thereby potentially indicating a higher CD4$^+$ T cell proliferative capacity for controls when stimulated by VZV lysate in comparison with HZ patients during HZ (Figure 1). We note that we can't exclude the potential presence of allo-antigens in the lysate, after the 1-week culture, which might have influenced this result. Furthermore, we also found a significantly lower CD4$^+$ T cell TCR count against the influenza-neuraminidase peptide (INFA-NA), which was included as a control for VZV specificity, during HZ compared to 1 year after the HZ episode (Figure 1).

HZ patients have a less diverse CD4$^+$ TCR repertoire against VZV gE and VZV IE63 peptide pools than controls after 1-week culture

Given that the total number of VZV peptide-pool-specific CD4$^+$ and CD8$^+$ T cells did not differ significantly between HZ patients and controls, we next questioned whether the diversity of the TCR repertoire could be a predictive factor for the development of HZ. Hereto, the Shannon's entropy (H) index, which takes into account the prevalence of each CDR3, was calculated for each sample of each group. The breadth type, reflecting the number of unique CDR3s per sample without taking into account its prevalence, was also determined (Figure S7), but this didn't show significant results. Since theoretically the TCR repertoire can be transiently upregulated during an HZ episode,[19] PBMCs from 23 convalescent HZ patients were primarily collected 1 year after the HZ episode (HZ1y) and around the same time point for 22 controls (CO). Additionally, PBMC from eight HZ patients were taken during the acute HZ episode. When considering the entire cohort, we found that the entropy index of CD4$^+$ T cell TCRs against VZV gE ($p = 0.019$) and VZV IE63 ($p = 0.038$) was statistically significantly lower in convalescent HZ patients

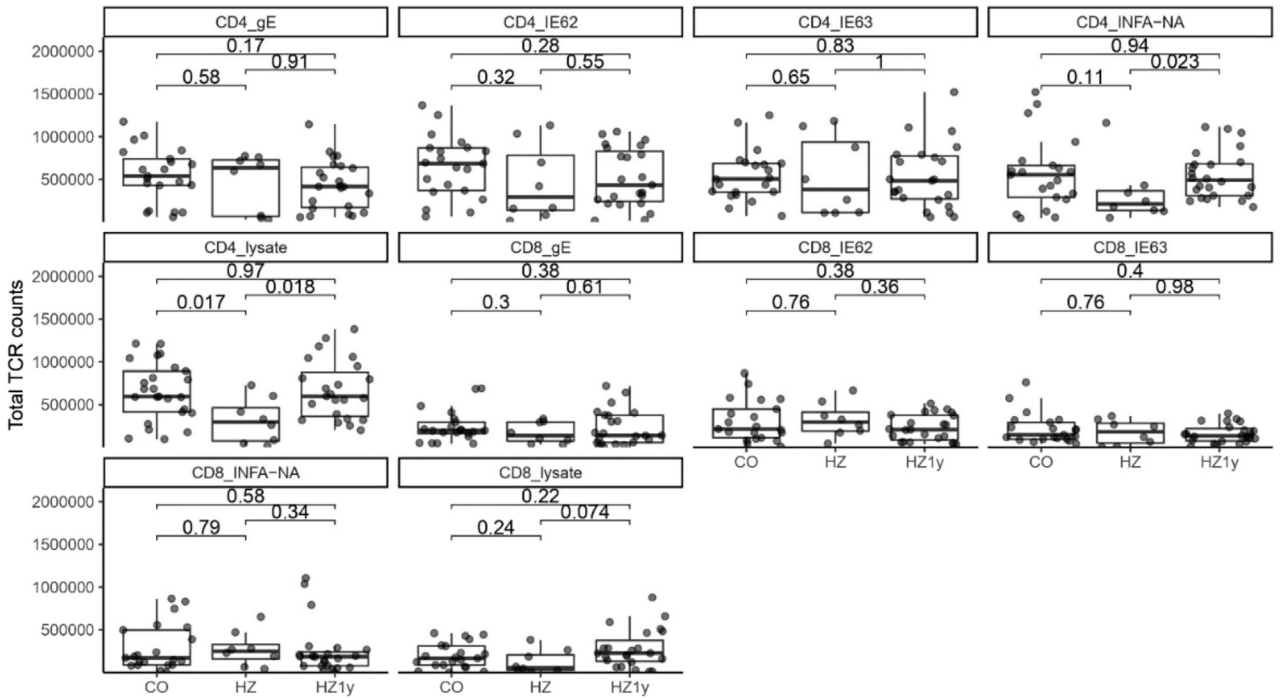

Figure 1. Total number of TCRs against VZV gE, VZV IE62, VZV IE63, VZV lysate, and a control peptide (INFA-NA)

The total number of sequenced CD4$^+$ and CD8$^+$ T cell TCRs against VZV IE62, VZV IE63, VZV gE, INA-NA (control peptide mix), and VZV lysate are shown, using median and interquartile range, in controls (CO: left boxplots) and in HZ patients during the active HZ episode (HZ: middle boxplots) and 1 year after HZ onset (HZ1y: right boxplots). The number of samples per group are 22 (CO), 8 (HZ), and 23 (HZ1y). Mann-Whitney U test with Bonferroni correction was used to calculate *p* values (shown on the graphs) between the groups.

(HZ1y) than controls (CO), indicating that HZ patients have a less diverse CD4$^+$ T cell TCR repertoire against VZV gE and IE63 peptides after 1-week culture (Figure 2A). Of note, the entropy index of CD4$^+$ T cell TCRs against VZV gE during the active HZ episode ($p = 0.0034$) was also significantly lower compared to controls (Figure 2A). Furthermore, in the subcohort aged 50 years or younger, the entropy index of CD4$^+$ T cell TCRs against VZV IE63 again was significantly lower ($p = 0.0056$) in HZ patients (HZ1y) than controls (CO), and the difference was even more pronounced than in the total cohort (Figure 2B). In contrast, in this subcohort, the entropy index of CD4$^+$ TCRs against VZV gE is only lower with a tendency for significance ($p = 0.051$) in HZ patients (HZ1y) compared with controls (CO) (Figure 2B). Lastly and unexpectedly, we found no significant differences in the diversity of the CD8$^+$ T cell TCR repertoire against any of the VZV peptides tested or the VZV lysate.

Ex vivo T cell dynamics show a decrease in VZV-associated TCR breadth following HZ

To further explore the T cell dynamics following HZ, we co-analyzed longitudinal TCRβ data from HZ patients from cohort 2 and controls from a previous study.[20] In brief, unstimulated CD8$^+$ T cells from six HLA-A02:01$^+$ individuals received TCR sequencing at different time points. Three individuals were sampled following HZ diagnosis, and three individuals were sampled following re-exposure to chickenpox (“EG” individuals). We deployed two independent strategies to track VZV-specific clonotypes across time points and to visualize the T cell dynamics. Firstly, the overlap was calculated between the longitudinal TCRβ data and the aforementioned CD8$^+$ VZV peptide-pool-specific TCRβ data (from cohort 1). We used the ClusTCR clustering tool to identify groups of similar sequences in the TCRβ data.[21] Secondly, two VZV epitope-specific TCRex annotation models, namely for HLA-A*02:01-IE62 (ALSQYHVYV) and HLA-A*02:01-ORF18 (ILIEGIFFV), were applied to the longitudinal TCRβ data. Both the overlap-based analysis and the IE62 model-based analysis indicated the same pattern of a decrease in VZV-associated TCR breadth following HZ and an increase in VZV-associated TCR breadth following secondary exposure (Figure S8). This pattern was not observed with the overlap with INFA CD8$^+$ TCRβ data (Figure S9) nor with the ORF18 TCRex model prediction (Figure S10). Notably, independent of the increase, the EG samples end with a higher VZV-associated breadth than the HZ samples.

T cells from convalescent HZ patients become less activated than those from controls after stimulation with VZV peptide pools

Besides VZV-specific TCR diversity, other VZV-specific T cell characteristics such as phenotype distribution, activation and expansion, and gene expression profile could also contribute to host susceptibility for HZ. To understand this better, single-cell sequencing (combining gene expression and TCR sequencing) was performed on T cells from nine HZ

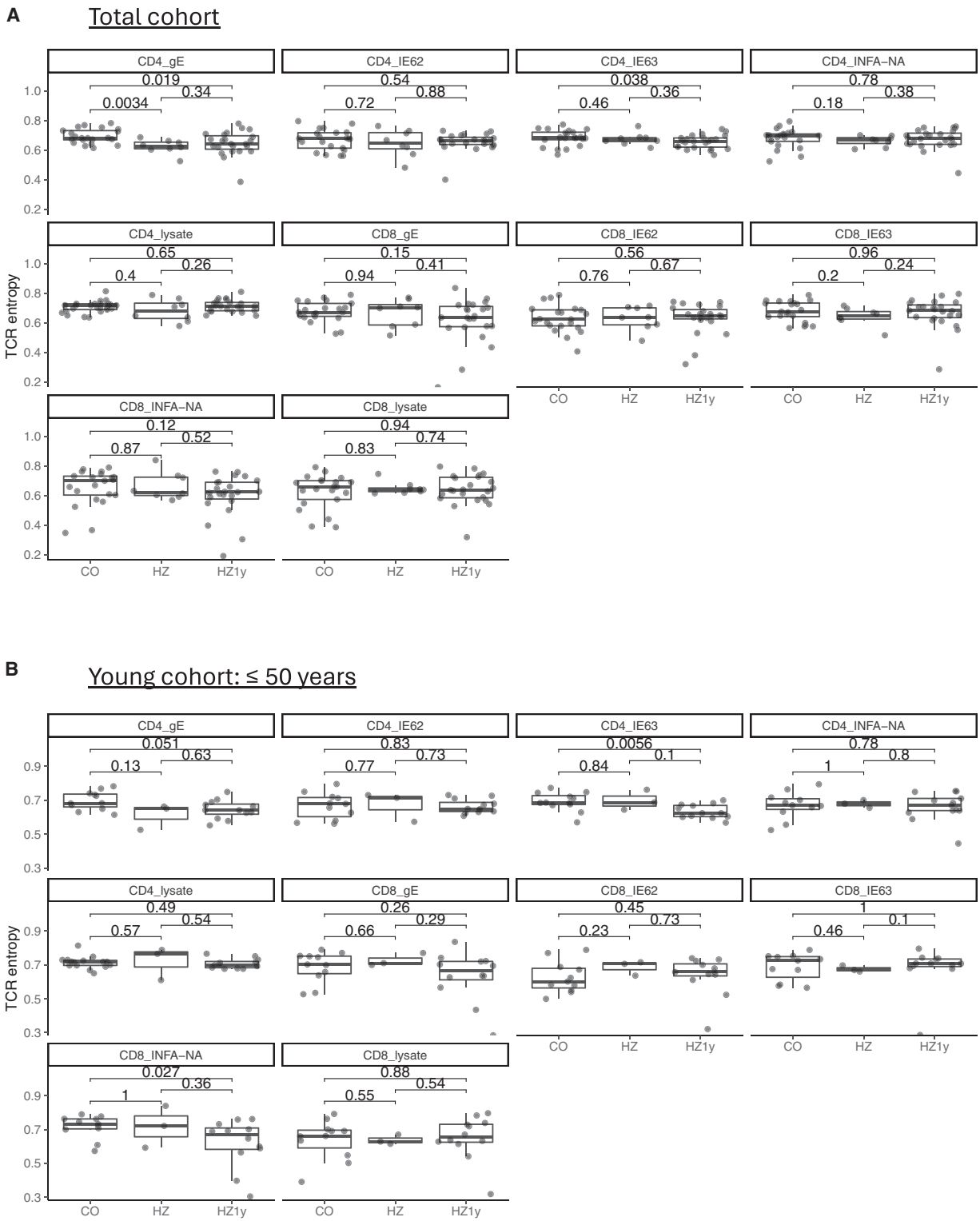

Figure 2. Diversity of the TCR repertoire in HZ patients and controls

(A) TCR entropy in the total cohort for $CD4^+$ and $CD8^+$ T cell TCRs against VZV IE62, VZV IE63, VZV gE, INFA-NA (control peptide mix), and VZV lysate are shown, using median and interquartile range, in controls (CO: left box pots) and in HZ patients during the active HZ episode (HZ: middle boxplots) and 1 year after HZ onset (HZ1y: right boxplots). The number of samples per group are 22 (CO), 8 (HZ), and 23 (HZ1y). Mann-Whitney U test with Bonferroni correction was used to calculate *p* values (shown on the graphs) between the groups.

(legend continued on next page)

patients 1 year after HZ and nine matched controls, after 16 h stimulation with VZV IE63 or VZV gE (Figure 3). First, we noted that the distribution of T cell phenotypes against each VZV peptide pool did not differ significantly between HZ patients and controls (Figures 3C, 3D, S11, and S12). Figure S13 (Figure S14 excluding CO15_1Y) shows the TCR counts per T cell phenotype (aggregated over VZV proteins), illustrating that most TCRs have little to no expansion in HZ patients and controls. In the largely expanded TCR regions, the presence of $CD8^+$ mucosal-associated T (MAIT) cells is noteworthy.

TCR breadth was determined for $CD4^+$ T cells and $CD8^+$ T cells separately and together (Figure 4). After the short stimulation (representing *ex vivo* frequencies) of T cells with VZV peptides, no significant differences in TCR breadth against VZV gE and IE63, between HZ patients 1 year after the HZ episode and controls, were found. Likely the fact that almost every TCR is uniquely present in each (small) sample from each individual hampers the power of our single-cell approach to confirm the reduced TCR diversity in HZ patients that we found after our 1-week culture. This hypothesis is supported by our longitudinal TCR mapping in HZ patients, which did show significant differences between HZ patients and re-exposed controls (see Figure S8).

Finally, to compare T cell activation pathways between HZ patients and controls, differentially expressed genes (DEGs) between HZ patients and controls were determined for $CD4^+$ T cells (Figure S15) and $CD8^+$ T cells (Figure 5). Interferon (IFN)-stimulated genes (ISGs) like IFI16, IFI35, IFI44, IFI44L, IFI6, IFIH1, IFIT1, IFIT2, IFIT3, ISG15, ISG20, Mx1, Mx2, OAS1, OAS2, OAS3, and OASL were all significantly downregulated in HZ patients compared to controls in $CD4^+$ T cells against VZV gE (Figure S15A) and VZV IE63 (Figure S15B) and in $CD8^+$ T cells against VZV IE63 (Figure 5B). This corresponds with a downregulation of the type I IFN response in $CD4^+$ T cells against VZV gE (Figure S15A) and VZV IE63 (Figure S15B) and in $CD8^+$ T cells against VZV IE63 (Figure 5B) in HZ patients versus controls. Furthermore, the IFNγ response was also downregulated in $CD4^+$ and $CD8^+$ T cells against VZV gE and IE63 from HZ patients compared to controls.

Given that these results could still be compatible with an overall reduced T cell activation, and thus not VZV specific, we divided the VZV-specific single cells into ''high-proliferation TCRs'' and ''low-proliferation TCRs.'' We did this by (1) redistributing the corresponding 1-week culture bulk TCR sequencing data on an individual-specific level in an above the median group and a below the median group regarding TCR abundance after 1-week culture (thereby reflecting proliferation capacity), (2) mapping the single-cell TCRs on these corresponding bulk TCR data per individual, and (3) comparing the DEGs between the cells bearing ''high-proliferation TCRs'' and the cells bearing ''low-proliferation TCRs'' (Figure 6). Using this approach, we show that the ''high-proliferation TCRs'' have a more activated gene expression profile than the ''low-proliferation TCRs'' of controls (Figure 6A), but that there is little difference between the high- and low-proliferation TCRs of HZ_1y participants (Figure 6B). In addition, high-proliferation TCRs from convalescent HZ patients showed less T cell activation pathway gene expression than the low-proliferation TCRs from controls (Figure S16). These findings are consistent with the concept that T cell proliferation and activation are significantly dominated by the TCR-epitope-MHC interaction. Our data are thus indicative of reduced interaction between HZ patients' TCRs and VZV epitopes leading to reduced T cell activation in HZ patients compared to controls.

$CD4^+$ TCR clustering shows increased participation of HZ TCRs in clustering and (pre-)HZ TCR co-clustering

Clustering of the V gene and CDR3 amino acid sequence was performed for VZV IE63 and VZV gE $CD4^+$ TCR repertoires from controls and convalescent HZ participants from cohort 1 individually using the ClusTCR algorithm.[21] Initially, participant CO15 was excluded from this analysis to reduce the effect on the clustering results. Next, we counted the number of TCRs originating from HZ and CO in each individual cluster. Binomial test (probability of success = 50%, corresponds to equal proportion of HZ/CO in the data) for every cluster to evaluate potential overrepresentation of HZ-originating TCRs, followed by multiple testing correction (Benjamini-Hochberg method), revealed no significant clusters for either VZV IE63 or VZV gE, thereby indicating the lack of overrepresentation of HZ or CO in certain TCR clusters.

In an alternative approach, we (1) clustered all TCRα and TCRβ sequences (for cohort 1 and cohort 3 separately), (2) calculated HZ/CO enrichment per cluster using a hypergeometric distribution, (3) selected the clusters with p value <0.05, (4) summed per individual the number of unique TCRs that participate in a ''corresponding group specific'' enriched cluster, and (5) compared HZ vs. CO using Mann-Whitney U test. For cohort 1, we did this for each individual VZV peptide (and $CD4^+$ and $CD8^+$ separately); see Figure S17. With this analysis, we aimed to show increased participation of TCRs in clustering for HZ or CO. Interestingly, this further confirmed that for VZV IE63 specific $CD8^+$ TCRs, VZV IE62 specific $CD4^+$ TCRs, and VZV gE specific $CD4^+$ TCRs, convalescent HZ patients showed significantly more participation in HZ-enriched TCR clusters than controls. The reverse was shown for VZV gE specific $CD8^+$ TCRs. Regarding the VZV lysate stimulation and $CD4^+$ T cells, convalescent HZ patients showed more co-clustering than controls (Figure S18). Next, we investigated $CD4^+$ T cells from pre-HZ and control participants (cohort 3) in two experimental settings. In setting 1, PBMCs from the 10 pre-HZ and 20 control participants were kept in the 1-week culture and VZV lysate specific T cells were again sorted via $CD71^+CD98^+$ gating. When TCR sequencing was performed, we noted that pre-HZ $CD4^+$ TCRs showed more co-clustering (Figure S19). These results suggest that after 1-week culture, pre-HZ patients and convalescent

(B) TCR entropy in the cohort of participants aged 50 or younger for $CD4^+$ and $CD8^+$ T cell TCRs against VZV IE62, VZV IE63, VZV gE, INFA-NA (control peptide mix), and VZV lysate are shown, using median and interquartile range, in controls (CO: left box pots) and in HZ patients during the active HZ episode (HZ: middle boxplots) and 1 year after HZ onset (HZ1y: right boxplots). The number of samples per group are 13 (CO), 3 (HZ), and 13 (HZ1y). Mann-Whitney U test with Bonferroni correction was used to calculate p values (shown on the graphs) between the groups.

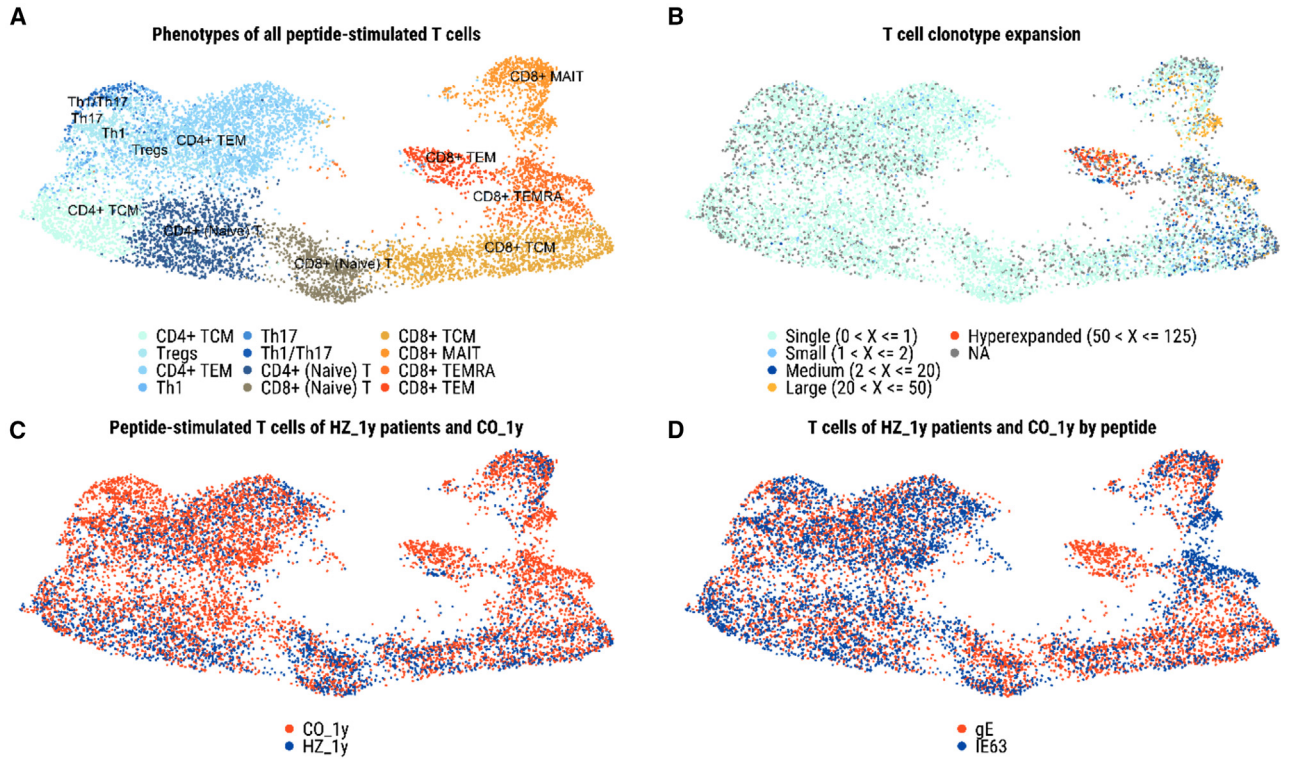

Figure 3. UMAP representation of the single T cells of HZ patients and controls showed no obvious difference in T cell phenotype distribution between HZ patients and controls

(A) The peptide-stimulated T cells of HZ patients and controls represented by gene expression-based phenotypes.

(B) Highlighting the cells with a linked TCR and their clonal expansion.

(C) The distribution of phenotypes and their phenotypes across the HZ and control groups.

(D) The distribution of cells and their phenotypes across the different VZV peptides. Results were obtained from nine HZ patients 1 year after the HZ episode (HZ_1Y) and nine age- and gender-matched controls (CO_1y). In Figure 3B, a cluster of hyperexpanded T cells, corresponding with the $CD8^+$ TEM cluster of Figure 3A, can be detected. It should be noted that this hyperexpanded region can be mainly attributed to one control (CO15_1y, Figure S11). We hypothesize (but cannot confirm) that this patient might have recently had a subclinical reactivation or unknown exogenous re-exposure to VZV.

HZ patients share more VZV epitopes recognized compared to controls, which likely indicates that a distinct target-epitope repertoire could be an HZ risk factor. In setting 2, PBMCs from the pre-HZ and CO participants were stimulated overnight with VZV lysate, and VZV lysate specific T cells were extracted via fluorescence-activated cell sorting using activation-induced markers ($CD154^+OX40^+CD4^+$ T cells). Interestingly, when considering pre-HZ vs. control *ex vivo* TCR co-clustering, controls showed more co-clustering than pre-HZ patients. This might indicate that at equilibrium (without VZV perturbations) controls share more VZV proteome recognition capacity.

Collectively, given the above results and given that absolute TCR counts didn't differ, we hypothesize that (pre-)HZ patients show a more restricted TCR repertoire after 1-week stimulation, potentially due to fewer TCRs that are capable to elicit an adequate proliferative response upon VZV lysate stimulation.

To look further into the above hypothesis, we assigned TCRs to two different categories for proliferation (high/low) based on their duplicate count in the 1-week culture experiments (cf. supra). Briefly, we used median TCR read count to delineate high-proliferating TCRs (> median) from low-proliferating TCRs (≤ median). Binomial testing showed no significant enrichment of high-proliferating clusters in either of the peptide-stimulated datasets.

Additionally, we sought to identify the differences between clustered and non-clustered T cell populations. We identified a higher tendency to cluster for HZ-originating TCRs compared to CO-originating TCRs. This effect was present in both VZV IE63 (p = 0.0026, Fisher's exact test) as well as VZV gE (p = 2.94e−15, Fisher's exact test). Additionally, we found that high-proliferating TCRs had a significantly smaller tendency to participate in clustering compared to the low-proliferating TCRs in both VZV IE63 (p = 1.05–208, Fisher's exact test) and VZV gE (p = 1.83e−145, Fisher's exact test). This leads us again to hypothesize that the increased participation of HZ TCRs in clustering is a hallmark for a decrease in response diversity (in terms of different epitopes they recognize).

VZV lysate specific $CD4^+$ TCR clustering suggests that pre-HZ TCRs target different epitopes than TCRs from controls

Given that the previous TCR high/low clustering analysis investigated the role of specific VZV proteins, we additionally looked into TCR high/low clustering from a VZV-whole-lysate perspective

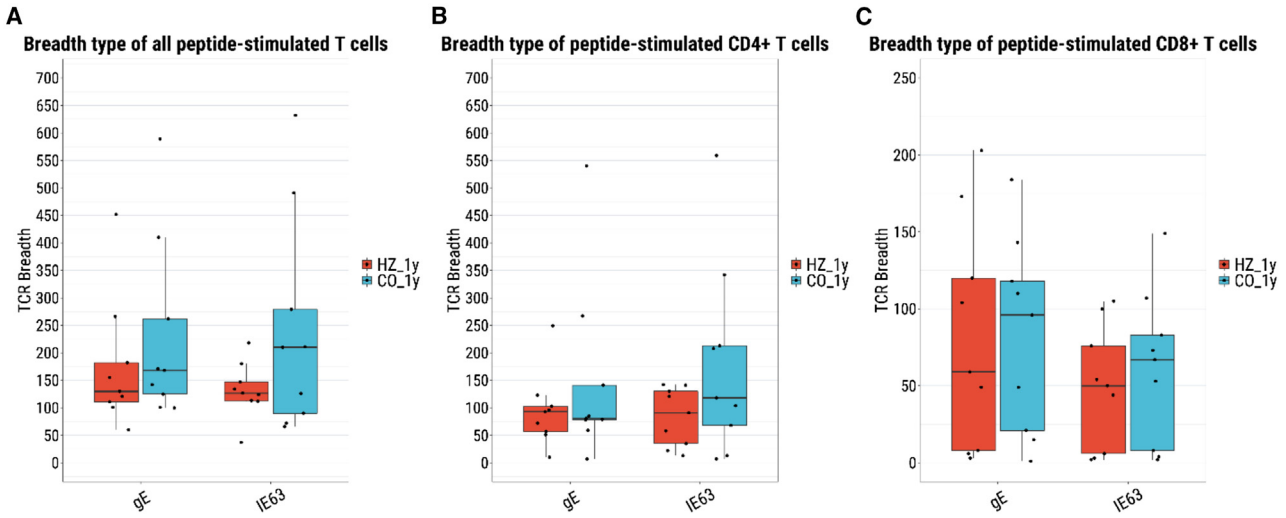

Figure 4. Single-cell TCR breadth of VZV-specific T cells after short-term stimulation did not differ significantly between HZ patients and controls

(A) Breadth type of all gE- and IE63-stimulated T cells across HZ patients and controls.

(B) Breadth type of gE- and IE63-stimulated CD4$^+$ T cells.

(C) Breadth type of gE- and IE63-stimulated CD8$^+$ T cells. Results were obtained from nine HZ patients 1 year after the HZ episode (HZ-1y) and nine age- and gender-matched controls (CO). For each group, the median with interquartile range is shown. Mann-Whitney U test with Bonferroni correction was used to calculate *p* values between the groups.

by performing TCR high/low clustering on TCR repertoire data obtained from PBMCs stimulated with VZV lysate. Given that previous results showed mainly a relevance for CD4$^+$ T cells, CD4$^+$ T cells were selected in further experiments.

First, we performed TCR clustering on the TCR data from VZV lysate stimulated PBMCs, cultured during 1 week, from cohort 1, and we applied the previously introduced high/low annotation. Interestingly, we didn't find fewer unique high-proliferation TCRs among convalescent HZ patients compared to controls (p = 0.642, t test); see Figures S20 and S21. Noteworthy, when adding all TCRs per group, HZ patients seem to have proportionally more high-proliferation TCRs compared to controls (p = 1.326e−85, chi-squared test). Overall, these results can't support the hypothesis that HZ patients would have a low-affinity CD4$^+$ TCR repertoire against the entire VZV lysate. We can only report the earlier found lower CD4$^+$ TCR affinity regarding specific VZV proteins.

Next, we investigated the pre-HZ and control participants (cohort 3). First, we noted the lack of difference in total TCR count and TCR breadth between pre-HZ and CO participants for the two settings (see Figure 7), although the total unique TCR count tended to be higher in CO vs. pre-HZ participants when looking at CD71$^+$CD98$^+$ data (p = 0.0556).

Next, using TCR clustering of overnight-stimulated T cells (by combining high/low-proliferation TCR data from cohort 1 and cohort 3 combined to increase power for the size-limited cohort 3), we noted that for low-proliferation TCRs, more unique TCRs were observed in CO participants compared to pre-HZ participants (p = 0.039); see Figure S22. Interestingly, TCRs from pre-HZ participants were proportionally found more among the high-proliferation TCRs than low-proliferation TCRs (p = 0.0023); see Figure S23. However, we note that these findings could lead to biased conclusions if we don't consider absolute TCR counts. If we aggregate clone counts on the TCR level and cluster clones from both CO and pre-HZ participants, we can evaluate whether the high-proliferation clones (from cohort 1 and cohort 3) co-cluster more often in CO and pre-HZ participants. From this approach, we can observe that the clustered low-proliferation TCRs originate proportionally less from CO repertoires compared to pre-HZ repertoires (p = 2.306e−106, Fisher's exact test).

Finally, if we look at clustering patterns of CO and pre-HZ among CD154$^+$OX40$^+$ TCRs, we can see that pre-HZ-originating TCRs cluster more often (together) than CO TCRs (p = 6.877e−07, Mann-Whitney U, Figure S24). This latter finding may suggest that pre-HZ TCRs target different epitopes than TCRs from CO participants.

Our analyses seem to support the concept that although TCR repertoires from (pre-)HZ patients were clearly defective against specific VZV proteins (at least the ones tested in our study), the overall TCR repertoire against the VZV lysate isn't defective in HZ patients compared to controls. Thus, we hypothesize that having a robust CD4$^+$ TCR repertoire against VZV IE62, VZV IE63, and gE might be more important in controlling VZV reactivation than having a broad CD4$^+$ TCR repertoire against the entire VZV lysate.

DISCUSSION

In this study, we show a link between the diversity and function of a pathogen-specific T cell receptor (TCR) repertoire and the host's potential for controlling (in particular reactivation of) an infectious disease in humans. Specifically, we showed that the CD4$^+$ TCR diversity, after 1-week culture after stimulation,

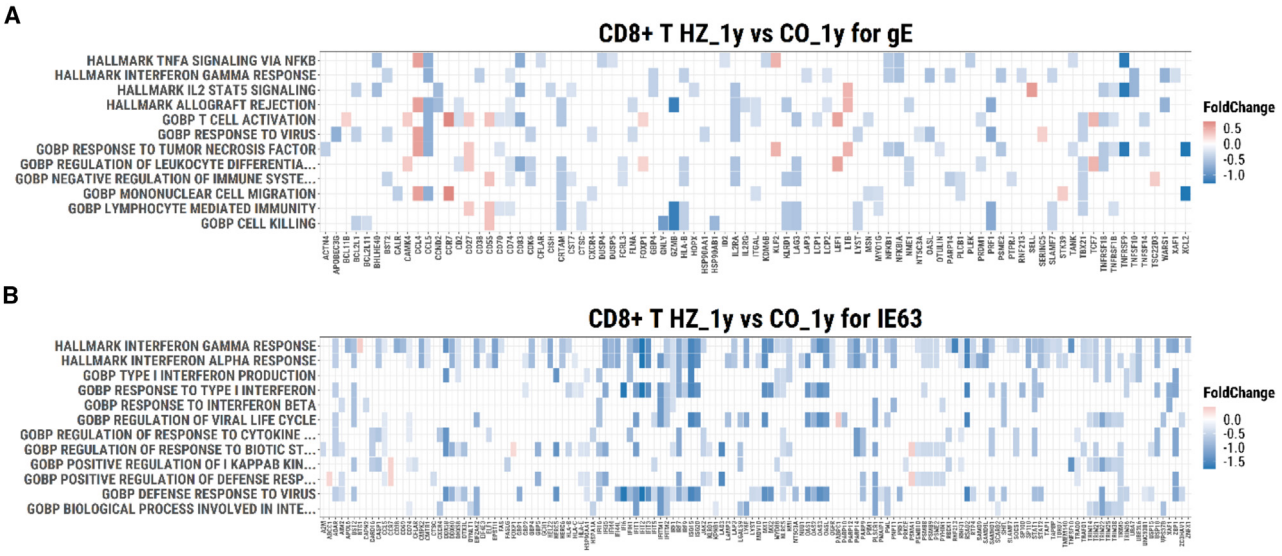

Figure 5. Pathway overrepresentation performed on the differentially expressed genes within the CD8$^+$ T cell compartment

(A) Differentially expressed genes between HZ patients and controls for the gE-stimulated CD8$^+$ T cells.

(B) Differentially expressed genes between HZ patients and controls for the IE63-stimulated CD8$^+$ T cells. Results were obtained from nine HZ patients 1 year after the HZ episode and nine age- and gender-matched controls.

against VZV peptides gE and IE63 was smaller in convalescent HZ patients than controls, thereby indicating that HZ patients have a lower range of VZV gE and VZV IE63 peptides that can be adequately ''recognized'' by T cells. In contrast to the live-attenuated HZ vaccine Zostavax in which the efficacy declines dramatically with age, the recombinant gE adjuvanted HZ vaccine Shingrix is over 90% effective in all age groups, including age groups $\geq$70 years and $\geq$80 years.[22,23] Noteworthy, currently Shingrix is only indicated for people aged 50 years or older and efficacy data in younger people is not available. Interestingly, the success of the Shingrix vaccine is mainly attributed to a strong CD4$^+$ T cell response against VZV gE.[24,25] This is fully in agreement with our data reporting that a low CD4$^+$ T cell TCR diversity against VZV gE could be a risk factor for the development of HZ in all age groups. Traditionally, however, induction of an adequate CD8$^+$ T cell response (rather than a CD4$^+$ T cell response) was associated with protection from disease due to viral infection and was the focus of vaccine development.[1] Furthermore, recent computational enrichment analyses predicted that of the six VZV genes known to be transcribed during VZV latency and important early in VZV reactivation, VZV IE4, IE62, and IE63 were depleted of high-affinity peptides across many HLA alleles coding for MHC I.[11–13] Unfortunately, in these reports, depletion of high-affinity peptides against HLA alleles related to MHC II was not studied. Recently, in a large GWAS, MHC II HZ risk loci were published.[14] Although we did not find a convincing significant difference in CD8$^+$ T cell TCR diversity against the VZV peptides IE62 or IE63 (IE4 peptides were not used in this study), we did find a smaller CD4$^+$ T cell TCR diversity against VZV IE63 in all age groups. We note that subclinical VZV reactivation was reported with reduced anti-VZV IE63 T cell responses in patients with malignancies.[26] When looking at the young subcohort of participants aged up to 50, the difference in CD4$^+$ T cell TCR diversity against VZV IE63 was even more pronounced, whereas differences in CD4$^+$ T cell TCR diversity against gE were less pronounced. Moreover, we did not detect major differences regarding VZV lysate specific CD4$^+$ TCRs between convalescent HZ patients and controls. Given that these results could be biased by the fact that the HZ PBMCs were obtained after HZ, we also sought and obtained PBMCs from individuals who developed HZ after PBMC isolation (+/− 1 to 18 months later). Interestingly, we didn't note major differences regarding different TCR metrics between participants prior to HZ development (pre-HZ) and controls.

Besides TCR diversity, we also determined T cell counts against VZV peptides on three cohorts using complementary methods. First, for cohort 1, we didn't detect differences between convalescent HZ and control participants in total number of TCRs of VZV peptide nor VZV lysate specific CD4$^+$ or CD8$^+$ T cells after 1-week culture. This lack of difference was further confirmed by an *ex vivo* AIM-based flow cytometric approach after VZV lysate and VZV IE63 stimulation. Next, for cohort 2, we analyzed the percentage of VZV-peptide-specific CD4$^+$ and CD8$^+$ T cells against VZV peptides IE62, IE63, and gE (after stimulation) by intracellular cytokine staining, from HZ onset up to 1 year after the HZ onset episode, and from control participants. This approach showed no significant differences in total T cell percentages of VZV-specific CD4$^+$ or CD8$^+$ T cells against VZV IE62, IE63, or gE peptides between any of the groups. We note that the Koelle lab recently noted a decline in VZV-proteome-specific CD4$^+$ T cell responses from day 45 after HZ onset to day 90 after HZ onset, which we couldn't replicate.[27] Potentially, their study was better powered to detect significant differences. Finally, our cohort 3, consisting of PBMCs obtained prior to the development of HZ, didn't show significant differences regarding VZV lysate nor VZV

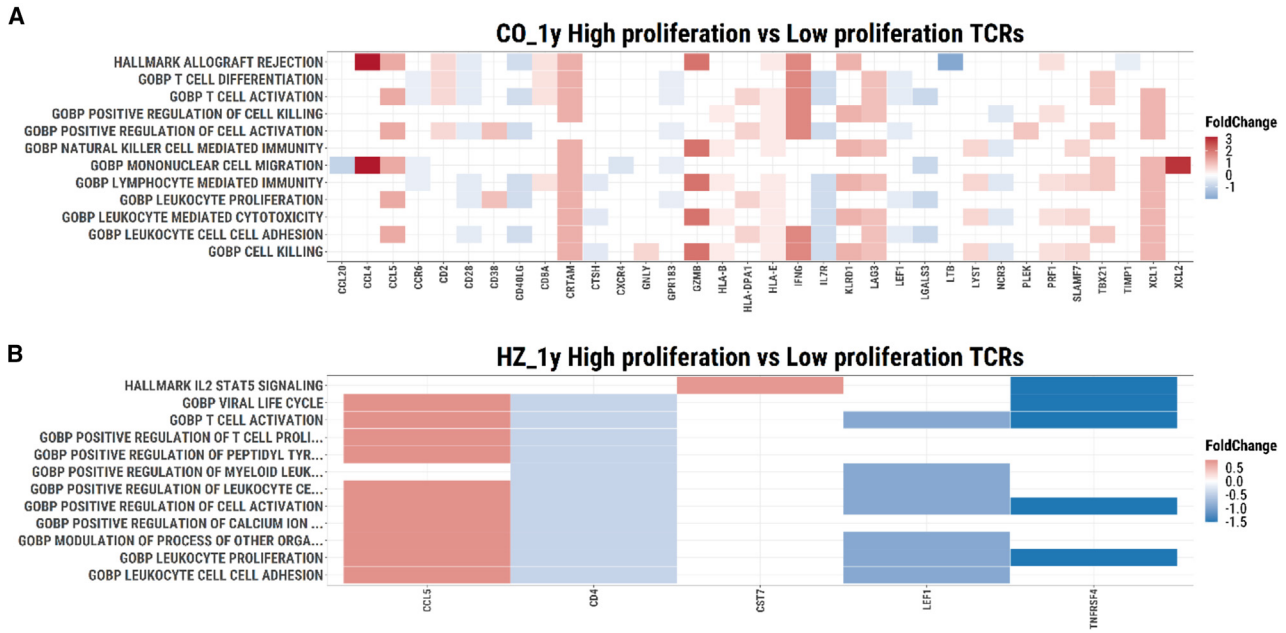

Figure 6. Pathway overrepresentation performed on the differentially expressed genes within the overlapping bulk- and single-cell TCRs

(A) Differentially expressed genes between high-proliferation and low-proliferation TCRs for the CO_1y participants.

(B) Differentially expressed genes between high-proliferation and low-proliferation TCRs for the HZ_1y participants. Results were obtained from nine HZ patients 1 year after the HZ episode and nine age- and gender-matched controls.

IE63 specific AIM-based T cell counts nor VZV lysate specific total TCR counts. Thus, based on these data, the total number of $CD4^+$ or $CD8^+$ T cells against VZV peptides and VZV lysate was, in contrast to TCR diversity, not suggested to be a risk factor for HZ. Surprisingly, we found a significantly lower total TCR count of $CD4^+$ T cells against the influenza-neuraminidase peptide (which was included as a control for VZV specificity), during the HZ episode compared to 1 year after the HZ episode. Whether there could be a relationship between HZ and a decline in circulating $CD4^+$ T cells against the influenza-neuraminidase peptide needs further investigation.

In addition, by investigating $CD4^+$ TCR clustering, we could look into the probability of HZ patients and controls sharing TCRs in clusters, which could be a sign of a shared epitope recognition capacity. Interestingly, overall, our TCR clustering analyses showed that TCRs from (pre-)HZ patients tend to co-cluster with TCRs from other (pre-)HZ patients more often than TCRs from controls with other controls. Together with the lack of differences between HZ patients and controls regarding absolute TCR counts, we are tempted to speculate that HZ is at least partially caused by a narrow VZV-specific TCR repertoire consisting of insufficient overlap with the VZV-specific TCR repertoire from controls (and in particular related to the tested VZV proteins).

Broad phenotyping of unstimulated PBMCs revealed no general differences in the percentage of monocytes, NK cells, DCs, B cells, $CD4^+$ or $CD8^+$ naive, EM, CM, or TEMRA T cells, during HZ and 1 year later, nor between samples taken 1 year after the HZ episode and controls, thereby suggesting that the host susceptibility for HZ is likely not characterized by a broader immune deficiency.

Single-cell sequencing on T cells stimulated by VZV IE63 or VZV gE (over 16 h) further confirmed the lack of overall differences in T cell phenotypes between HZ patients and controls. Importantly, however, we did see that both type I and type II interferon-stimulated gene expression pathways (and other T cell activation pathways) were significantly lower expressed in HZ patients than controls. We hypothesize that this indicates that not only *ex vivo* VZV-specific TCR diversity is lower in HZ patients, but likely the VZV-specific TCRs from HZ patients elicit a lower activation upon stimulation by VZV peptide pools due to lower functional TCR-peptide interaction. This hypothesis was further supported by the finding that in controls, T cell clones that proliferated more vigorously after a week-long culture upon VZV stimulation had significantly more upregulated T cell activation pathways after short-term VZV stimulation.

In conclusion, our findings showed an unanticipated reduced $CD4^+$ T cell TCR repertoire diversity against VZV IE63 and gE, which is of great interest for a better understanding of the underlying pathophysiology and the mode of action of protection elicited by HZ vaccination. In addition, we showed that the existing VZV-specific TCRs in HZ patients likely bared a too low functional interaction with important VZV proteins, thereby eliciting a low T cell activation.

Importantly, we showed a link between not only the diversity of the TCRs but the functional interaction with the pathogen-derived proteins too and the risk for the reactivation of an infectious disease in humans. The same strategy could be applied for other (acute, chronic, and latent) infectious diseases, providing insights into virus pathophysiology and leads for vaccine development.

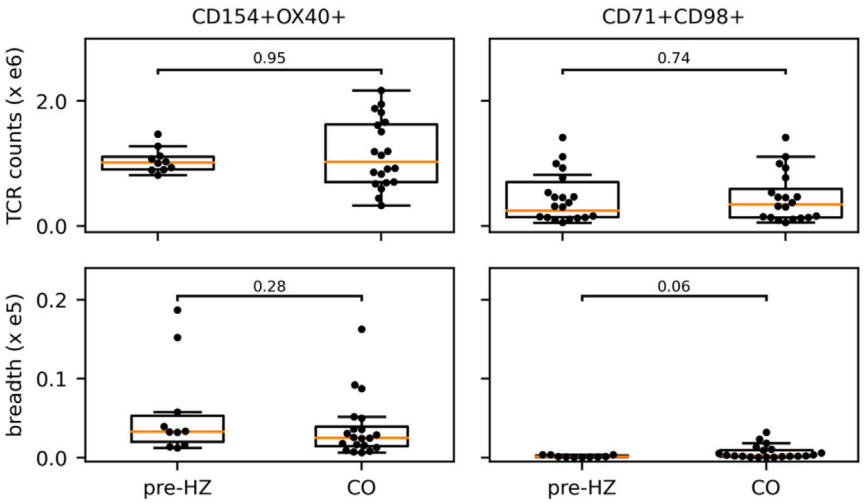

Figure 7. Total TCR counts and TCR breadth for culture (CD154+OX40+) and overnight-stimulated (CD71+CD98) samples across cohort 3 subjects

No differences were observed between pre-HZ and CO participants in terms of total TCR counts. There was a slight tendency for increased TCR breadth (i.e., broader functional response) among CO participants compared to pre-HZ ($p = 0.0556$). Pre-HZ: individuals who will develop HZ.

Limitations of the study

Our study is, despite the significant results, limited by the sample size of each study group. Furthermore, we only included peptide mixes against VZV gE, IE62, and IE63 in this study, while total TCR counts and TCR diversity against other VZV peptides may also be of importance, which might be illustrated by some results related to TCR diversity after stimulation with the VZV lysate. In addition, our work did not include a thorough analysis of the potential association of the TCR alpha chain with the occurrence of HZ.

STAR★METHODS

Detailed methods are provided in the online version of this paper and include the following:

- KEY RESOURCES TABLE
- RESOURCE AVAILABILITY
  - Lead contact
  - Materials availability
  - Data and code availability
- EXPERIMENTAL MODEL AND STUDY PARTICIPANT DETAILS
- METHOD DETAILS
  - Blood processing
  - Mass cytometry
  - Flow cytometric analyses and T cell sorting
  - RNA extraction and TCR sequencing
  - Mapping VZV-specific TCRs on longitudinally obtained $CD8^+$ TCRs from HZ patients
  - Single-cell sequencing
  - Antibody titration
  - AIM-based T cell phenotyping
- QUANTIFICATION AND STATISTICAL ANALYSIS

SUPPLEMENTAL INFORMATION

Supplemental information can be found online at https://doi.org/10.1016/j.celrep.2024.114062.

ACKNOWLEDGMENTS

We appreciate the participation of all patients in this study. We thank Steven Heynderickx, Carole Faghel, and Kristof Bergs for their work in the lab. We thank Vincent Van Deuren for the discussions. We thank Geert Mortier for his support. We are grateful to all unmentioned clinicians, nurses, and lab colleagues. We thank Dr. Sofie Van Gassen and Professor Yvan Saeys for their help with FLOWSOM. With support from the "Universitaire Stichting van België."

The following funding sources are acknowledged: Research Foundation Flanders (FWO) 1S71721N (N.d.V.); Research Foundation Flanders (FWO) 11D1612N (B.O.); Research Foundation Flanders (FWO) G040912N (P.B., N.H., E.S., P.V.D.); Research Foundation Flanders (FWO) G067118N (K.L.; B.O.; P.D.; V.V.T.), Research Foundation Flanders (FWO) 1S48819N (S.G.); Research Foundation Flanders (FWO) 1244321N (S.V.); Research Foundation Flanders (FWO) 1861219N (B.O.); Research Foundation Flanders (FWO) 1S40321N (S.V.); Research Foundation Flanders (FWO) G034721N (P.P., P.D., B.O.); Hercules Foundation Flanders, University of Antwerp predoctoral fellowship (J.V.D.B.); University of Antwerp concerted research action (P.B., V.V.T., P.V.D.); University of Antwerp Methusalem VAXINFECTIO funding (P.P., P.V.D., N.H.); University of Antwerp Excellence Center ASCID (P.B., P.V.D.); University of Antwerp Excellence Center Infla-Med (P.P.); University of Antwerp Scientific chair of Evidence-based vaccinology (N.H.); University of Antwerp IOF POC 46947 (M.B., P.D., P.P., B.O.); iBOF Modulating Immunity and the Microbiome for Effective CRC Immunotherapy (MIMICRY) Project (K.L.); and European Union's Horizon 2020 research and innovation programme grant agreement 851752-CELLULO-EPI (B.O.).

AUTHOR CONTRIBUTIONS

Conceptualization: B.O. Design: M.B., N.d.V., M.K.H., A.S., S.V., S.G., N.V., S.V., N.H., E.S., P.V.D., P.B., P.P., V.V.T., P.D., K.L., P.M., and B.O. Recruitment, study management, and experimentation: M.B., M.K.H., M.K., J.S., E.B., J.V.D.B., N.M., O.A., J.L., A.B., J.L., E.L., J.W., K.P., M.-P.E., H.J., and B.O. Data analysis: M.B., N.d.V., M.K.H., S.V., A.S., S.G., and P.M. Funding acquisition: N.d.V., S.V., S.G., S.V., N.H., E.S., P.V.D., P.G.T., P.B., P.P., V.V.T., P.D., K.L., and B.O. Supervision: E.B., G.E., W.A., A.S., N.H., E.S., P.V.D., P.G.T., P.B., V.V.T., K.L., P.M., and B.O. Writing: M.B., N.d.V., M.K.H., S.V., A.S., M.K., S.G., J.S., E.B., J.V.D.B., N.M., O.A., J.L., A.B., J.L., E.L., J.W., K.P., M.-P.E., G.E., N.V., H.J., W.A., A.S., S.V., N.H., E.S., P.V.D., P.G.T., P.B., P.P., V.V.T., P.D., K.L., P.M., and B.O.

DECLARATION OF INTERESTS

K.L., P.M., and B.O. are co-founders, board directors, and shareholders of ImmuneWatch. None of the work presented here was influenced in any way

by this. ImmuneWatch had no role in study design, data collection and analysis, decision to publish, or preparation of the manuscript.

Received: February 17, 2023
Revised: February 23, 2024
Accepted: March 21, 2024

REFERENCES

1. Abul Abbas, A.H.L., and Pillai, S. (2019). Basic Immunology (Elsevier).
2. Gattorno, M., and Martini, A. (2005). CHAPTER 3 - THE IMMUNE SYSTEM AND THE INFLAMMATORY RESPONSE. In Textbook of Pediatric Rheumatology, Fifth Edition, J.T. Cassidy, R.E. Petty, R.M. Laxer, and C.B. Lindsley, eds. (W.B. Saunders), pp. 19–63. https://doi.org/10.1016/B978-1-4160-0246-8.50009-7.
3. Blum, J.S., Wearsch, P.A., and Cresswell, P. (2013). Pathways of Antigen Processing. Annu. Rev. Immunol. *31*, 443–473. https://doi.org/10.1146/annurev-immunol-032712-095910.
4. Boeren, M., Meysman, P., Laukens, K., Ponsaerts, P., Ogunjimi, B., and Delputte, P. (2023). T cell immunity in HSV-1- and VZV-infected neural ganglia. Trends Microbiol. *31*, 51–61. https://doi.org/10.1016/j.tim.2022.07.008.
5. Kawai, K., Gebremeskel, B.G., and Acosta, C.J. (2014). Systematic review of incidence and complications of herpes zoster: towards a global perspective. BMJ Open *4*, e004833. https://doi.org/10.1136/bmjopen-2014-004833.
6. Levin, M.J., Smith, J.G., Kaufhold, R.M., Barber, D., Hayward, A.R., Chan, C.Y., Chan, I.S.F., Li, D.J.J., Wang, W., Keller, P.M., et al. (2003). Decline in varicella-zoster virus (VZV)-specific cell-mediated immunity with increasing age and boosting with a high-dose VZV vaccine. J. Infect. Dis. *188*, 1336–1344. https://doi.org/10.1086/379048.
7. Ogunjimi, B., Smits, E., Hens, N., Hens, A., Lenders, K., Ieven, M., Van Tendeloo, V., Van Damme, P., and Beutels, P. (2011). Exploring the impact of exposure to primary varicella in children on varicella-zoster virus immunity of parents. Viral Immunol. *24*, 151–157. https://doi.org/10.1089/vim.2010.0031.
8. Dolin, R., Reichman, R.C., Mazur, M.H., and Whitley, R.J. (1978). Herpes Zoster-Varicella Infections in Immunosuppressed Patients. Ann. Intern. Med. *89*, 375–388. https://doi.org/10.7326/0003-4819-89-3-375.
9. Bilcke, J., Ogunjimi, B., Marais, C., de Smet, F., Callens, M., Callaert, K., van Kerschaver, E., Ramet, J., van Damme, P., and Beutels, P. (2012). The health and economic burden of chickenpox and herpes zoster in Belgium. Epidemiol. Infect. *140*, 2096–2109. https://doi.org/10.1017/s0950268811002640.
10. Ogunjimi, B., Buntinx, F., Bartholomeeusen, S., Terpstra, I., De Haes, I., Willem, L., Elli, S., Bilcke, J., Van Damme, P., Coenen, S., and Beutels, P. (2015). Herpes zoster is associated with herpes simplex and other infections in under 60 year-olds. J. Infect. *70*, 171–177. https://doi.org/10.1016/j.jinf.2014.08.016.
11. Meysman, P., Ogunjimi, B., Naulaerts, S., Beutels, P., Van Tendeloo, V., and Laukens, K. (2015). Varicella-zoster virus-derived major histocompatibility complex class I-restricted peptide affinity is a determining factor in the HLA risk profile for the development of postherpetic neuralgia. J. Virol. *89*, 962–969. https://doi.org/10.1128/jvi.02500-14.
12. Meysman, P., De Neuter, N., Bartholomeus, E., Elias, G., Van den Bergh, J., Emonds, M.P., Haasnoot, G.W., Heynderickx, S., Wens, J., Michels, N.R., et al. (2018). Increased herpes zoster risk associated with poor HLA-A immediate early 62 protein (IE62) affinity. Immunogenetics *70*, 363–372. https://doi.org/10.1007/s00251-017-1047-x.
13. Meysman, P., Fedorov, D., Van Tendeloo, V., Ogunjimi, B., and Laukens, K. (2016). Immunological evasion of immediate-early varicella zoster virus proteins. Immunogenetics *68*, 483–486. https://doi.org/10.1007/s00251-016-0911-4.
14. Vandoren, R., Boeren, M., Schippers, J., Bartholomeus, E., Mullan, K., Michels, N., Aerts, O., Leysen, J., Bervoets, A., Lambert, J., et al. (2024). Unravelling the immune signature of herpes zoster: Insights into pathophysiology and the HLA risk profile. J. Infect. Dis. jiad609. https://doi.org/10.1093/infdis/jiad609.
15. Stervbo, U., Nienen, M., Weist, B.J.D., Kuchenbecker, L., Hecht, J., Wehler, P., Westhoff, T.H., Reinke, P., and Babel, N. (2019). BKV Clearance Time Correlates With Exhaustion State and T-Cell Receptor Repertoire Shape of BKV-Specific T-Cells in Renal Transplant Patients. Front. Immunol. *10*, 767. https://doi.org/10.3389/fimmu.2019.00767.
16. Levin, M.J., Oxman, M.N., Zhang, J.H., Johnson, G.R., Stanley, H., Hayward, A.R., Caulfield, M.J., Irwin, M.R., Smith, J.G., Clair, J., et al. (2008). Varicella-zoster virus-specific immune responses in elderly recipients of a herpes zoster vaccine. J. Infect. Dis. *197*, 825–835. https://doi.org/10.1086/528696.
17. Ogunjimi, B., Hens, N., Pebody, R., Jansens, H., Seale, H., Quinlivan, M., Theeten, H., Goossens, H., Breuer, J., and Beutels, P. (2015). Cytomegalovirus seropositivity is associated with herpes zoster. Hum. Vaccin. Immunother. *11*, 1394–1399. https://doi.org/10.1080/21645515.2015.1037999.
18. Ogunjimi, B., Theeten, H., Hens, N., and Beutels, P. (2014). Serology indicates cytomegalovirus infection is associated with varicella-zoster virus reactivation. J. Med. Virol. *86*, 812–819. https://doi.org/10.1002/jmv.23749.
19. Qi, Q., Cavanagh, M.M., Le Saux, S., NamKoong, H., Kim, C., Turgano, E., Liu, Y., Wang, C., Mackey, S., Swan, G.E., et al. (2016). Diversification of the antigen-specific T cell receptor repertoire after varicella zoster vaccination. Sci. Transl. Med. *8*, 332ra46. https://doi.org/10.1126/scitranslmed.aaf1725.
20. Ogunjimi, B., Van den Bergh, J., Meysman, P., Heynderickx, S., Bergs, K., Jansens, H., Leuridan, E., Vorsters, A., Goossens, H., Laukens, K., et al. (2017). Multidisciplinary study of the secondary immune response in grandparents re-exposed to chickenpox. Sci. Rep. *7*, 1077. https://doi.org/10.1038/s41598-017-01024-8.
21. Valkiers, S., Van Houcke, M., Laukens, K., and Meysman, P. (2021). ClusTCR: a python interface for rapid clustering of large sets of CDR3 sequences with unknown antigen specificity. Bioinformatics *37*, 4865–4867. https://doi.org/10.1093/bioinformatics/btab446.
22. Lal, H., Cunningham, A.L., Godeaux, O., Chlibek, R., Diez-Domingo, J., Hwang, S.J., Levin, M.J., McElhaney, J.E., Poder, A., Puig-Barberà, J., et al. (2015). Efficacy of an adjuvanted herpes zoster subunit vaccine in older adults. N. Engl. J. Med. *372*, 2087–2096. https://doi.org/10.1056/NEJMoa1501184.
23. Cunningham, A.L., Lal, H., Kovac, M., Chlibek, R., Hwang, S.-J., Díez-Domingo, J., Godeaux, O., Levin, M.J., McElhaney, J.E., Puig-Barberà, J., et al. (2016). Efficacy of the Herpes Zoster Subunit Vaccine in Adults 70 Years of Age or Older. N. Engl. J. Med. *375*, 1019–1032. https://doi.org/10.1056/NEJMoa1603800.
24. Cunningham, A.L., Heineman, T.C., Lal, H., Godeaux, O., Chlibek, R., Hwang, S.-J., McElhaney, J.E., Vesikari, T., Andrews, C., Choi, W.S., et al. (2018). Immune Responses to a Recombinant Glycoprotein E Herpes Zoster Vaccine in Adults Aged 50 Years or Older. J. Infect. Dis. *217*, 1750–1760. https://doi.org/10.1093/infdis/jiy095.
25. Weinberg, A., and Levin, M.J. (2010). VZV T cell-mediated immunity. Curr. Top. Microbiol. Immunol. *342*, 341–357. https://doi.org/10.1007/82_2010_31.
26. Malavige, G.N., Rohanachandra, L.T., Jones, L., Crack, L., Perera, M., Fernando, N., Guruge, D., and Ogg, G.S. (2010). IE63-specific T-cell responses associate with control of subclinical varicella zoster virus reactivation in individuals with malignancies. Br. J. Cancer *102*, 727–730. https://doi.org/10.1038/sj.bjc.6605542.
27. Laing, K.J., Ouwendijk, W.J.D., Campbell, V.L., McClurkan, C.L., Mortazavi, S., Elder Waters, M., Krist, M.P., Tu, R., Nguyen, N., Basu, K., et al. (2022). Selective retention of virus-specific tissue-resident T cells in healed

skin after recovery from herpes zoster. Nat. Commun. *13*, 6957. https://doi.org/10.1038/s41467-022-34698-4.

28. Quintelier, K., Couckuyt, A., Emmaneel, A., Aerts, J., Saeys, Y., and Van Gassen, S. (2021). Analyzing high-dimensional cytometry data using FlowSOM. Nat. Protoc. *16*, 3775–3801. https://doi.org/10.1038/s41596-021-00550-0.
29. Elias, G., Ogunjimi, B., and Van Tendeloo, V. (2019). Tracking Dye-Independent Approach to Identify and Isolate In Vitro Expanded T Cells. Cytometry A. *95*, 1096–1107. https://doi.org/10.1002/cyto.a.23867.
30. Gielis, S., Moris, P., Bittremieux, W., De Neuter, N., Ogunjimi, B., Laukens, K., and Meysman, P. (2019). Detection of Enriched T Cell Epitope Specificity in Full T Cell Receptor Sequence Repertoires. Front. Immunol. *10*, 2820. https://doi.org/10.3389/fimmu.2019.02820.
31. Stoeckius, M., Zheng, S., Houck-Loomis, B., Hao, S., Yeung, B.Z., Mauck, W.M., Smibert, P., and Satija, R. (2018). Cell Hashing with barcoded antibodies enables multiplexing and doublet detection for single cell genomics. Genome Biol. *19*, 224. https://doi.org/10.1186/s13059-018-1603-1.
32. Hao, Y., Hao, S., Andersen-Nissen, E., Mauck, W.M., Zheng, S., Butler, A., Lee, M.J., Wilk, A.J., Darby, C., Zager, M., et al. (2021). Integrated analysis of multimodal single-cell data. Cell *184*, 3573–3587.e29. https://doi.org/10.1016/j.cell.2021.04.048.
33. Becht, E., McInnes, L., Healy, J., Dutertre, C.-A., Kwok, I.W.H., Ng, L.G., Ginhoux, F., and Newell, E.W. (2018). Dimensionality reduction for visualizing single-cell data using UMAP. Nat. Biotechnol. *37*, 38–44. https://doi.org/10.1038/nbt.4314.
34. Aran, D., Looney, A.P., Liu, L., Wu, E., Fong, V., Hsu, A., Chak, S., Naikawadi, R.P., Wolters, P.J., Abate, A.R., et al. (2019). Reference-based analysis of lung single-cell sequencing reveals a transitional profibrotic macrophage. Nat. Immunol. *20*, 163–172. https://doi.org/10.1038/s41590-018-0276-y.
35. Andreatta, M., Berenstein, A.J., and Carmona, S.J. (2022). scGate: marker-based purification of cell types from heterogeneous single-cell RNA-seq datasets. Bioinformatics *38*, 2642–2644. https://doi.org/10.1093/bioinformatics/btac141.
36. Phipson, B., Sim, C.B., Porrello, E.R., Hewitt, A.W., Powell, J., and Oshlack, A. (2022). propeller: testing for differences in cell type proportions in single cell data. Bioinformatics *38*, 4720–4726. https://doi.org/10.1093/bioinformatics/btac582.
37. Wu, T., Hu, E., Xu, S., Chen, M., Guo, P., Dai, Z., Feng, T., Zhou, L., Tang, W., Zhan, L., et al. (2021). clusterProfiler 4.0: A universal enrichment tool for interpreting omics data. Innovation *2*, 100141. https://doi.org/10.1016/j.xinn.2021.100141.
38. Liberzon, A., Birger, C., Thorvaldsdóttir, H., Ghandi, M., Mesirov, J.P., and Tamayo, P. (2015). The Molecular Signatures Database Hallmark Gene Set Collection. Cell Syst. *1*, 417–425. https://doi.org/10.1016/j.cels.2015.12.004.
39. Borcherding, N., Bormann, N.L., and Kraus, G. (2020). scRepertoire: An R-based toolkit for single-cell immune receptor analysis. F1000Res. *9*, 47. https://doi.org/10.12688/f1000research.22139.2.
40. Whyte, C.E., Tumes, D.J., Liston, A., and Burton, O.T. (2022). Do more with Less: Improving High Parameter Cytometry Through Overnight Staining. Curr. Protoc. *2*, e589. https://doi.org/10.1002/cpz1.589.

STAR★METHODS

KEY RESOURCES TABLE

REAGENT or RESOURCE	SOURCE	IDENTIFIER
Antibodies		
See Table S1		
See Table S2		
Biological samples		
Peripheral blood mononuclear cells		
Chemicals, peptides, and recombinant proteins		
INFA-NA	JPT	C7FH14
VZV gE	JPT	P09259
VZV IE62	JPT	Q8AZM1
VZV IE63	JPT	Q77NN7-1
VZV lysate	Microbix	EL-03-02
Critical commercial assays		
Quick-RNA Microprep Kit	Zymo Research	R1050
QIAseq Immune Repertoire RNA Library Kit	Qiagen	333705
Chromium Next GEM Single Cell 5' Reagent Kits v2 (Dual Index)	10x Genomics	CG000330
Deposited data		
Bulk TCR-seq data		https://doi.org/10.5281/zenodo.7445684
Oligonucleotides		
See Table S3		
See Table S4		
TotalSeq™-C 0251 anti-human Hashtag 1	BioLegend	394661
TotalSeq™-C 0252 anti-human Hashtag 2	BioLegend	394663
TotalSeq™-C 0253 anti-human Hashtag 3	BioLegend	394665
TotalSeq™-C 0254 anti-human Hashtag 4	BioLegend	394667
TotalSeq™-C 0255 anti-human Hashtag 5	BioLegend	394669
TotalSeq™-C 0256 anti-human Hashtag 6	BioLegend	394671
Software and algorithms		
FlowSOM	Ghent University	https://doi.org/10.1038/s41596-021-00550-0
FlowJo	BD Biosciences	flowjo.com
MiXCR	MiLaboratories Inc	https://doi.org/10.1038/nmeth.3364mixcr.com
TCRex	University of Antwerp	https://doi.org/10.3389/fimmu.2019.02820
ClusTCR	University of Antwerp	https://doi.org/10.1093/bioinformatics/btab446
CellRanger	10x Genomics	10xgenomics.com/support/software/cell-ranger/latest
Python	Python Software Foundation	python.org
R	R Foundation	r-project.org

RESOURCE AVAILABILITY

Lead contact

Further information and requests for resources and reagents should be directed to and will be fulfilled by the lead contact, Benson Ogunjimi (benson.ogunjimi@uantwerpen.be).

Materials availability

This study did not generate new unique reagents.

Data and code availability

- Bulk TCR-seq data have been deposited at Zenodo and are publicly available as of the date of publication. The DOI is listed in the key resources table.
- All original code is publicly available as of the date of publication. DOIs are listed in the key resources table.
- Any additional information required to reanalyze the data reported in this work paper is available from the lead contact upon request.

EXPERIMENTAL MODEL AND STUDY PARTICIPANT DETAILS

A first cohort (cohort 1, see Figure S25) of 26 HZ patients aged between 18 years and 70 years (median age 51 years; 13 men, 13 women) were prospectively recruited during an active HZ episode (median days between onset of HZ and sampling: 9 days, range: 3–37 days; based on available information from 23 of the 26 HZ patients), as confirmed by a positive VZV PCR on skin swab, saliva or blood (EDTA) or by significantly elevated (>4 times) VZV IgG titers. The exclusion criteria were: (i) auto-immune disease, immunosuppressed state or immunocompromised state due to disease or medication (e.g., use of systemic prednisolone or equivalent >20 mg/day for more than two weeks in the last six months; intra-articular, inhalation and topical steroids were allowed), (ii) invasive malignancy <20y prior to the study, (iii) serious disorders of coagulation, (iv) any condition that the investigator believed might interfere with the study. We were able to obtain serum (kept in −80°C) and PBMC (Lithium-Heparin, Ficoll) from eight of the included HZ patients during the acute episode, via standard procedures, and PBMC were cryopreserved. A second blood collection was done approximately one year after the HZ episode (23 out of the initial 26 HZ participants: 11 men, 12 women), during which serum and PBMC were stored. Age- (±1 birth year) and gender-matched controls without a history of HZ were recruited for each HZ patient and time of donated blood around the one-year timepoint (considered to be a proxy for the "baseline"). Three of these controls also donated blood one year earlier around the same time as blood collection from their matched HZ patient during the active HZ episode (Figure S25).

A second cohort (cohort 2) of 12 HZ patients (median age 56.5 years; 5 men, 7 women) were prospectively recruited after VZV PCR confirmation on saliva swab or skin swab or after VZV IgG elevation and longitudinally sampled during HZ (T0: 10 participants), +/− 3 weeks (T3: 9 participants), +/− 6 weeks (T6: 11 participants), +/− 15 weeks (T15: 11 participants) and +/− 30 weeks (T30: 7 participants) after HZ onset. Eleven (age- and gender-matched) controls, without known re-exposure to VZV in the last year and without a history of HZ, contributed a single blood sample (Figure S25).

A third cohort (cohort 3) included 10 pre-HZ participants whose blood had been collected and processed 1–18 months before they developed HZ, as well as 20 age- and gender-matched controls (thus, two controls per pre-HZ participant) without known VZV–re-exposure or HZ history.

This study was approved by the ethics board of the Antwerp University Hospital & University of Antwerp (Belgian registration numbers B300201112798, B300201734433 and B3002020000019). All methods were performed in accordance with the relevant guidelines and regulations when applicable. Written informed consent was obtained from all study participants.

METHOD DETAILS

Blood processing

PBMCs were isolated by either (cohort 1 and cohort 2) Ficoll-Paque Plus gradient separation (Amersham Biosciences) or Lymphoprep separated (cohort 3) (Stemcell) from freshly obtained heparinized blood. PBMCs were frozen in 90% fetal bovine serum (FBS, Life Technologies) supplemented with 10% dimethyl sulphoxide (DMSO; Sigma-Aldrich). Filled cryovials were placed in Corning CoolCell LX Cell Freezing Containers before freezing at −80°C, and after 24 h, the cells were stored in liquid nitrogen.

Mass cytometry

After thawing, PBMC from cohort 1 were stained with surface markers (Table S1) following the Maxpar Cell Surface Staining with Fresh Fix Protocol (Fluidigm, USA). Briefly, cells were washed with PBS to remove excess stimulants and then stained with 103Rh isotope (Fluidigm, USA) for viability. Subsequently, cells were stained with the surface markers listed in Table S1 for 30 min at RT. After incubation, cells were washed with PBS and fixed with 1.6% formaldehyde for 10 min at RT. Next, cells were stained with Cell-ID Intercalator-Ir in Maxpar Fix and Perm Buffer (Fluidigm, USA) for 1h at RT, then spun-down and resuspended in the residual volume after the supernatant was discarded. Cells were cryopreserved at −80°C until measurement. Prior to measurement, cells were washed and resuspended in Cell Acquisition Solution (Fluidigm, USA). Calibration beads (Fluidigm, USA) were added for normalization. Cells were then filtered into strainer-capped tubes and samples were analyzed on the Helios instrument (Fluidigm, USA).

For data analysis, FlowSOM, a clustering algorithm for visualization and analysis of cytometry data, was used as described in Nature Protocols, Quintelier et al. 2021.[28] In short, the FlowSOM analysis procedure consists of: (i) loading of the pre-processed data (doublet removal, compensation and transformation, removal of low-quality measurements, testing for batch effects, creation of an aggregate), (ii) training of a FlowSOM model, (iii) evaluation of the quality of the model, (iv) interpretation of the results. As input data, normalized Flow Cytometry Standard (FCS) files and a vector of the column names specifying the channels, was used. Random

points from the input data were used for the initialization of a self-organizing map (SOM), i.e., a grid of nodes representing the points. The SOM was trained and visualized by a minimum spanning tree connecting all the nodes with their most similar ones. A second, higher-level, clustering was performed to end up with meta-clusters, giving the most consistent grouping according to the multiple subsampling iterations. To ensure the quality of the output, 2D scatterplots of the clusters were inspected and correspondence with manual gating labels was verified. The FlowSOM model was used for relative quantification of the cell populations in each sample and to compare between groups.

Flow cytometric analyses and T cell sorting

Regarding cohort 1: 1 million PBMCs were, after thawing, either unstimulated (DMSO control) or stimulated in AIM V medium +5% FBS with 2.5μg/mL of VZV IE62 PepMix, VZV IE63 PepMix, VZV gE PepMix or influenza A-neuraminidase (INFA-NA) PepMix (control peptide mix) or 0.28 mg/mL of VZV lysate (Strain VZ-10, Microbix, Canada). All peptide mixes were purchased from JPT (Berlin, Germany) and consisted of 15-mer peptides with an 11-aa overlap. At day 3 or 4 medium was topped up to 1mL to avoid exhaustion of cell medium. At day 7, cells were washed and stained using antibodies for flow cytometry (Table S2). Right before analysis, SYTOX blue nucleic acid stain (Invitrogen) was added to stain dead cells. Live activated $CD8^+$ T cells ($CD3^+$ $CD4^-$ $CD8^+$ $CD71^{high}CD98^{high}$) and $CD4^+$ T cells ($CD3^+$ $CD4^+$ $CD8^-$ $CD71^{high}CD98^{high}$) were separately sorted in DNA/RNA shield (Zymo Research) and frozen at −20°C (Figure S26: gating strategy). The assay used to identify and sort *in vitro* expanded T cells was previously published by our group in Cytometry, Elias et al. 2019.[29] Percentages of proliferated T-cells after stimulation are shown in Figure S27. Flow cytometric analyses and cell sorting were performed on a BD FACSAria II flow cytometer (BD Biosciences). FlowJo software (BD Biosciences) was used for data analysis.

Regarding cohort 2: stimulation of PBMCs with VZV and control peptides was described and published in Scientific Reports, Ogunjimi et al. 2017.[20]

Regarding cohort 3: 1 million PBMCs were, after thawing, either unstimulated (DMSO control) or stimulated in AIM-V medium (supplemented with 5% FBS) with 0.28 mg/mL of VZV lysate (strain VZ-10, Microbix, Canada). For each sample, two cultures were prepared separately: overnight stimulation and one-week expansion. For overnight stimulation, $CD154^+OX40^+CD4^+$ T-cells were sorted. For one-week expansion, $CD71^{high}CD98^{high}CD4^+$ T-cells were sorted. The staining panel was as follows: CD3 – VioBlue, CD4 – PE/Vio770, CD8 – APC, CD154 – PE, OX40 – FITC, CD98 – PE, CD71 – FITC, viability – NIR. Sorting was performed on a BD FACSAria II flow cytometer (BD Biosciences). Sorted cells were stored in DNA/RNA shield (Zymo Research) at −20°C for subsequent RNA extraction and TCR sequencing.

RNA extraction and TCR sequencing

T cells stored in DNA/RNA shield (Zymo Research) were thawed at RT and processed using the Quick-RNA microprep kit (R1050, Zymo Research) following the manufacturer's instructions. Eluted RNA was stored at −80°C for subsequent TCRβ sequencing. TCRβ library for sequencing was constructed by the QIAseq Immune Repertoire RNA Library Kit (Qiagen), pooled and sequenced on a NextSeq 500 with the Qiaseq read 1 custom primer (NextSeq v2.5 Mid Output 300 cycles, asymmetric 261-41 paired-end Illumina). VDJ alignment and read counting was performed using MiXCR v3.0.7. The TCR data were converted to the V, D and J assignments, the CDR3 length distribution, clustering, total, breadth and Shannon entropy index. The Shannon index is a measure of immune diversity ranging between 0 and 1, where 1 indicates the most diversity and 0 indicates a fully clonal population.

Mapping VZV-specific TCRs on longitudinally obtained $CD8^+$ TCRs from HZ patients

DNA from three HZ patients (cohort 2) and three controls (grandparents who were re-exposed to chickenpox via their grandchild) was extracted from 200,000 $CD8^+$ T cells per subject at baseline (HZ onset or exposure to chickenpox), +/− 6 weeks later and +/− 30 weeks later (see Ogunjimi et al., 2017). TCRβ sequencing was performed by Adaptive Biotechnologies. Few shared T cell clonotypes can be expected between these longitudinal TCR repertoires and VZV-associated T cells extracted from other individuals, therefore two independent strategies were employed to identify VZV-associated TCR sequences in the longitudinal TCRβ data using *in silico* models. The overlap-based analysis (strategy 1) clustered all TCRβ sequenced from the $CD8^+$ T cell peptide-mix stimulated samples (from cohort 1, cf. supra) with each longitudinal TCRβ data in turn using the clusTCR tool v1.0.2.[21] This results in a set of clusters of TCRβ sequences based on their amino acid similarity. Those clusters that grouped TCRβ sequences from both the longitudinal samples and the stimulated samples were retained for further analysis. In addition, only those clusters were retained that were specific to a peptide-mix from a single protein. The specificity of a cluster was determined based on the presence of at least 2 TCRβ from at least one or more stimulation samples against one of the proteins, and at most one against any of the other antigens. The VZV-associated breadth per sample was then calculated as the number of longitudinal TCRβ present in those clusters that were determined to be specific against one of the VZV antigens (gE, IE62, IE63).

The model-based analysis (strategy 2) was performed using the TCRex webtool (v0.3.2)[30] trained on tetramer-stained VZV epitopes from IE62 (ALSQYHVYV, HLA-A*02:01) and ORF18 (ILIEGIFFV, HLA-A*02:01). Data are available on https://tcrex.biodatamining.be or Tables S3 and S4. In brief, TCRex trains a machine learning model to identify the antigen specificity of unseen TCRβ sequences based on common patterns identified within other TCRβ sequences that have been found to bind the same epitope. The model-based breadth consisted of the number of unique TCRβ sequences with a BPR score below or equal to the default BPR

cut-off (0.01%), which estimates the likelihood of getting a prediction with identical or higher decision values in a background dataset of TCRβ sequences.

Single-cell sequencing

Cells sorted from 36 samples stimulated by VZV IE63 or gE PepMix (9 patients plus 9 age- and gender-matched controls) were selected for the single-cell sequencing experiments. Per condition, approximately 2 million PBMC were stimulated with a peptide mix and after 16 h, sorting was performed by gating on the activation-induced markers CD154 and OX40 for antigen-responsive $CD4^+$ T cells, and CD137 and CD69 for antigen-responsive $CD8^+$ T cells using a BD FACSAria II flow cytometer (BD Biosciences) (Figure S28: gating strategy). After being sorted (see Figure S29 for cell numbers), cells were stained with oligo-tagged anti-human CD4, CD8, and six hashtag antibodies (BioLegend) for multiplexing.[31] Next, six samples with distinct hashtags were pooled, making two pools per batch in two batches. Oligo-stained cells and barcoded gel beads were loaded onto Chromium Next GEM Chip K (10× Genomics, catalog no. 1000287) and partitioned in oil droplets using the Chromium Controller (10× Genomics). Cell concentration was adjusted to 100–200 cells/μL before loading to target 2000–4000 recovered cells. All subsequent steps were performed based on the Chromium Next GEM Single Cell 5′ Dual Index v2 protocol (10× Genomics, catalog no. CG000330). Libraries were pooled and sequenced on the Illumina NovaSeq 6000 obtaining average read depths of approximately 120,000 reads per cell for gene expression libraries, around 20,000 reads per cell for surface proteins (CD4, CD8, and hashtags) and V(D)J-enriched T cell libraries.

The *multi* pipeline of the Cell Ranger version 7.0.1 software was used to demultiplex the hashed 5′ gene expression FASTQ library, assigning reads to individual samples. Next, the resulting sample-specific BAM files were converted back to FASTQ files, using the *bamtofastq* function of the Cell Ranger software. A final run of the *multi* pipeline was performed to map the sample-specific gene expression FASTQ library reads to the GRCh38 reference genome, while simultaneously aligning the reads from the V(D)J library to the V(D)J-compatible GRCh38 7.0.0 reference set and generating the antibody feature barcode count matrix. The resulting gene expression and antibody count matrices were analyzed using the Seurat package version 4.1.0[32] in the R programming language version 4.2. The data of individual samples were integrated using Seurat's *merge* command, and subsequently inspected to confirm for a lack of batch effects. To remove multiplets and other low-quality cells, all cells expressing <500 and >5000 genes were filtered out. For the same purpose, only cells expressing below 10% mitochondrial gene counts and above 5% ribosomal gene counts were included. The data was then log-transformed, scaled, and centered. Next, the 2.000 most variable genes were identified and used as input for a principal component analysis. The top 16 principal components were then used for clustering, and for dimension reduction and visualization using the Uniform Manifold Approximation and Projection (UMAP) method.[33] The resulting cell clusters were annotated using an ensemble method of reference-based mapping based on the SingleR package version 1.8.0,[34] and with a gating strategy as employed by the scGate package version 1.0.0.[35] The propeller method of the speckle package version 0.99.1[36] was used to test for differences in cell type proportions across the different groups. Differentially expressed genes (DEGs) were identified using the *FindMarkers* function in Seurat with the default Wilcoxon Rank-Sum test. A $\log_2$ fold change threshold of 0.25 was applied, and only genes with a Benjamini-Hochberg adjusted p value of <0.05 were considered for further analysis. The identified DEGs were subjected to over-representation analysis using the clusterProfiler package,[37] and the top 12 enriched pathways were visualized using the enrichplot package. Gene sets used include the Hallmark (H) and GO ('C5') categories from the MSigDB 7.4.[38] The scRepertoire package version 1.7.2[39] was used to integrate the TCR data with the gene expression and antibody data. Clonotypes were defined as the unique combination of V(D)J genes and the CDR3 nucleotide sequence. The breadth was then calculated as the number of unique clonotypes per sample, without taking into account their prevalence.

Antibody titration

Serum was stored at −80°C until further processing as described in Scientific Reports, Ogunjimi et al. 2017.[20] VZV-specific IgG antibody titers (mIU/mL) in thawed serum were determined using VZV-infected cell lysate on a Liaison XL instrument with a DiaSorin kit.[20] The presence of IgGs directed against CMV pp150, pp28, p38, and p52 in thawed serum was determined using a Roche Elecsys assay.[20]

AIM-based T cell phenotyping

PBMCs from cohorts 1–3 were, after thawing, either unstimulated (DMSO control) or stimulated for 24 h in AIM-V medium (supplemented with 5% FBS) with 2.5μg/mL of VZV IE63 PepMix (JPT, Germany) or 0.28 mg/mL of VZV lysate (Strain VZ-10, Microbix, Canada). Next, cells were stained with viability dye (near-IR) for 30 min, fixed in 4% paraformaldehyde for 15 min, and then stained overnight (using the Whyte et al. protocol[40]) with fluorescent antibodies (CD154 – VioBright B515, CD69 – BB700, CCR7 – APC, CD3 – VioBright R720, CD45 – VioGreen, CD27 – BV570, CD137 – BV605, TIGIT – BV650, CD28 – BV711, CD45RA – BV786, LAG3 – PE, Fas – PE/Vio615, OX40 – PE/Cy5, CD4 – PE/Cy5.5, CD8 – PE/Vio770). Data acquisition was performed on Novocyte Quanteon (Agilent).

QUANTIFICATION AND STATISTICAL ANALYSIS

Statistical analyses were performed using JMP (SAS), SPSS v27. (IBM) or GraphPad Prism v8.2.1. For the TCRβ sequencing results, RStudio (2021.09.0) with R4.1.1 was used and statistical analysis was performed using ggpubr v0.4.0. TCR clustering was performed

using the ClusTCR package (1.0.2) in python (3.8.12). The statsmodels (0.13.3) and scipy (1.7.3) packages were used for downstream statistical analysis of the TCR clustering results. The matploplib (3.6.2) library was used for plotting. For all T cell enumeration experiments where stimuli (peptides or lysate) were used unstimulated frequencies were subtracted from the stimulated frequencies.

The results were termed significant if the multiple testing corrected (Bonferroni) p value was < 0.05. Given the nonnormal distribution of the data and limited sample size, Mann-Whitney U test was used to compare medians between responses of HZ patients (at different timepoints) and controls, and Wilcoxon matched-pair signed rank test was used to compare medians from HZ patients at different timepoints. Fisher's Exact Test was used for contingency table analysis.